Translational Oncology 51 (2025) 102202

Contents lists available at ScienceDirect

Translational Oncology

journal homepage: www.elsevier.com/locate/tranon

Original Research

# The 7-Methylguanosine (m7G) methylation METTL1 acts as a potential biomarker of clear cell renal cell carcinoma progression

Yi Liu [a,b,1], Yanji Zhan [a,1], Jiao Liu [a,c,1], Zhengze Shen [d,1], Yudong Hu [a], Ling Zhong [a], Yuan Yu [a], Bin Tang [a,*], Jing Guo [e,*]

[a] Department of Nephrology, Second Affiliated Hospital, Chongqing Medical University, Chongqing, 400010, China
[b] The 3rd Affiliated Hospital, Chengdu Medical College, Chengdu Pidu District People's Hospital, Chengdu, 611730, China
[c] Department of Nephrology, Wushan County People's Hospital of Chongqing, 404700, China
[d] Department of Pharmacy, Yongchuan Hospital of Chongqing Medical University, Chongqing, 402160, China
[e] Radiation Oncology Center, Chongqing University Cancer Hospital, Chongqing University, Chongqing 400030, China

ARTICLE INFO

*Keywords:*
METTL1
7-methylguanosine (m7G)
Clear cell renal cell carcinoma
Prognosis
Tumor immune microenvironment

ABSTRACT

**Background:** Clear cell renal cell carcinoma (ccRCC) is the most common subtype of renal cancer. 7-Methylguanosine (m7G), one of the most prevalent RNA modifications, has been reported to play an important role in ccRCC progression; however, the specific regulators of m7G modification that are involved in this function remain unclear. This study aimed to explore the correlation between regulators of m7G methylation and ccRCC progression using unsupervised machine learning methods.

**Methods:** Transcriptome and clinical data of ccRCC were retrieved from The Cancer Genome Atlas (TCGA) database to identify differentially expressed m7G-related genes associated with the overall survival of patients with ccRCC. To construct and validate a prognostic risk model, TCGA dataset samples were divided into training and test sets. A multiple-gene risk signature was constructed using least absolute shrinkage and selection operator Cox regression analysis, and its prognostic significance was assessed using Cox regression and survival analyses. Finally, immunohistochemistry was performed to verify the prognostic significance of this signature.

**Results:** In total, 537 patients with ccRCC were included in this study. We found that 26 m7G RNA methylation regulators that were significantly differentially expressed. Univariate and multifactorial Cox regression analyses revealed that METTL1 expression was associated with ccRCC progression.

**Conclusions:** METTL1 associated with m7G may serve as a potential biomarker for ccRCC prognosis and diagnosis. Moreover, it may affect the prognosis of ccRCC by regulating the tumor immune microenvironment, providing a potential therapeutic target for immunotherapy. These results provide a new perspective on the role of M7G-related RNAs in ccRCC pathogenesis.

## Background

Clear cell renal cell carcinoma (ccRCC) ranks as the most predominant subtype within renal cell carcinoma (RCC) [1,2]. Despite the benefits conferred by early surgery or ablative strategies in improving patient survival rates, up to one-third of patients eventually develop metastases, with a quarter experiencing recurrent metastasis following curative surgical resection [3]. In ccRCC, lactotransferrin, an important protein in the innate immune system, is downregulated and promotes metastatic growth. Interestingly, this downregulation also enhances the response to mammalian target of rapamycin (mTOR) inhibitors in ccRCC tumor cells, suggesting that it could serve as a predictive biomarker for therapeutic effectiveness [4]. Previous studies have demonstrated that the 5-year relative survival rate for early stage ccRCC is 75.2 % [5], whereas that for stage IV ccRCC remains below 10 % [6]. Consequently, making an early diagnosis and precise prognostic estimation is paramount importance [7].

The 7-methylguanosine (m7G), one of the most prevalent RNA modifications, has been identified as part of the mRNA 5' cap structure, as well as in human ribosomal RNA (rRNA), transfer RNA (tRNA), and

* Corresponding authors.
*E-mail addresses:* tangbin@hospital.cqmu.edu.cn (B. Tang), guojingcoco@cqu.edu.cn (J. Guo).
[1] The authors contributed equally to this study.

https://doi.org/10.1016/j.tranon.2024.102202
Received 4 May 2024; Received in revised form 30 September 2024; Accepted 11 November 2024

microRNA [8–10]. Recent studies have shown that m7G methylation is closely associated with the tumorigenesis and progression of various cancers [11–13]. For instance, in prostate cancer, recent studies have shown that protein kinase B (AKT)/mTOR downstream signaling pathways regulate methyltransferase-like 1 (METTL1) expression and that METTL1 overexpression promotes tumorigenesis through the biogenesis of tRNA fragments [14]. Similarly, in breast cancer, METTL1-mediated modification of tRNA m7G plays a crucial tumor-suppressive role by facilitating the translation of growth arrest and DNA damage-inducible 45 alpha and RB transcriptional corepressor 1 mRNA, which specifically interfere with cell cycle progression during the G2/M phase [15]. Furthermore, studies have found that the WD repeat domain 4 (WDR4) component of the m7G methyltransferase complex mediates translation of cyclin B1 mRNA by enhancing its binding to eukaryotic translation initiation factor 2A, thereby promoting the progression of hepatocellular carcinoma [16]. In addition, overexpression of the m7G regulator METTL1/WDR4 increases the expression of cell cycle progression genes, thus promoting tumor formation in acute myeloid leukemia [17]. Moreover, the WBSCR22/TRMT112 methyltransferase complex, which writes the m7G modification at a specific G1639 location in 18S rRNA, has been reported to activate oxaliplatin-induced apoptosis in colon cancer [18]. These findings across various cancer types highlight the diverse and significant roles of m7G methylation in cancer biology. However, research on the relationship between the regulators of m7G modification and tumor progression is still at the preliminary stage, particularly in clear cell renal cell carcinoma (ccRCC).

Given the critical role of m7G modification in various cancers and the lack of comprehensive studies on its effect in ccRCC, this study aims to investigate the impact of m7G regulatory genes on ccRCC progression and prognosis. Specifically, we identify associations between m7G regulator genes and the clinical characteristics of ccRCC using consensus clustering analysis. Moreover, we construct a prognostic model to estimate ccRCC progression based on m7G regulatory gene expression. In addition, we investigate the correlation of the key m7G regulatory gene METTL1 with clinicopathological features, biological functions, signaling pathways, and drug sensitivity in ccRCC. By addressing these objectives, we aim to provide a comprehensive understanding of the role of m7G modification in ccRCC and potentially uncover novel biomarkers and therapeutic targets for this aggressive malignancy.

## Materials and methods

### *Data acquisition*

The Cancer Genome Atlas Kidney Renal Clear Cell Carcinoma (TCGA-KIRC) mRNA FPKM transcriptome data and associated clinical information were downloaded from the TCGA database (https://portal.gdc.cancer.gov/projects/TCGA-KIRC). A database of 72 normal samples and 537 ccRCC samples with gene expression and clinical information was retrieved by matching the sample ID. These datasets were also used to analyze the expression profiles of genes associated with m7G and to perform a prognostic assessment of patients with ccRCC based on the analysis. Patients without missing clinical and pathological characteristic data were excluded, and the average of repeated gene expression data from the same patient was calculated. The downloaded raw data were preprocessed using Perl software (version strawberry-perl-5.32.1-64bit), and the extracted matrix was analyzed using bioinformatics procedures on R software (version 4.1.0). This study did not require ethical approval because the data were obtained from a publicly accessible database.

### *Patient inclusion and exclusion criteria*

The clinical and transcriptome data of the patients were downloaded from TCGA (Project ID: TCGA-KIRC). Patients without follow-up clinical or transcription data were excluded, as previously reported [19]. The inclusion criteria for human ccRCC tissue samples were as follows: samples obtained from patients aged 18-80 years [20]; and histologically confirmed ccRCC. The exclusion criteria were samples obtained from patients with missing clinical and follow-up data.

### *Gene selection*

Given the emerging evidence of methylguanosine's crucial role in cancer progression and its potential as a source of novel biomarkers and therapeutic targets, we focused our investigation on methylguanosine-related genes. To systematically identify relevant methylguanosine-related genes, we searched the gene set enrichment analysis (GSEA) database (www.gsea-msigdb.org/gsea/index.jsp) for methylguanosine-related genes and obtained three gene sets (GOMF_M7G_5_PPPN_DIPHOSPHATASE_ACTIVITY, GOMF_RNA_7_METHYLGUANOSINE_CAP_BINDING, and GOMF_RNA_CAP_BINDING). After removing duplicated genes, 34 m7G-related genes remained: METTL1, WDR4, NSUN2, DCP2, DCPS, NUDT1, NUDT10, NUDT11, NUDT16, NUDT16L1, NUDT3, NUDT4, NUDT4B, NUDT5, NUDT7, AGO2, CYFIP1, CYFIP2, EIF4E, EIF4E1B, EIF4E2, EIF4E3, GEMIN5, LARP1, NCBP1, NCBP2, NCBP3, EIF3D, EIF4A1, EIF4G3, IFIT5, LSM1, NCBP2L, and SNUPN.

### *Identification of differentially expressed genes*

Differentially expressed genes (DEG) of the m7G regulator between normal and tumoral tissues were determined using Wilcoxon test of the 'limma' (version 3.58.1) package with a cut-off criterion of $p<0.05$. The correlations between these genes were evaluated using the R package 'corrplot' (version 0.92).

### *Hierarchical clustering for m7G-related methylation genes*

The 'ConsensusClusterPlus' package (version 1.66.0) [21] was used for consensus clustering with k = 2–9. A cluster heatmap was drawn using the 'pheatmap' package. The cumulative distribution function (CDF) values were compared with the clustering results. Additionally, we tested the relationship between clustering and prognosis using Kaplan-Meier curves and clinical factors.

### *Principal component analysis*

To verify the clustering of the results, principal component analysis (PCA) was performed using the 'limma' package and visualized using the 'ggplot2' package.

### *Least absolute shrinkage and selection operator prognostic modeling*

The Least Absolute Shrinkage and Selection Operator (LASSO) Cox regression analysis was used to mitigate the risk of model overfitting. LASSO regression is particularly effective for high-dimensional data because it applies a penalty to the regression coefficients, thereby reducing the number of variables included in the model [22,23]. The penalty parameter lambda was determined through cross-validation using the R package 'glmnet' (version 4.1-8). This method is widely used owing to its ability to increase the prediction accuracy and enhance interpretability by selecting the most relevant features from a large set of predictors [24].

Univariate Cox and LASSO regression analyses were used to construct a prognostic signature by screening genes associated with survival in the derived population cohort. For each patient with ccRCC, the risk score was calculated using the following formula:

Risk score $= \sum_{i=1}^{n} expi * \beta i$ where $n$ represents the number of prognostic genes, $expi$ the expression level of prognostic gene $i$, and $\beta i$ the regression coefficient of gene $i$. The downloaded TCGA database was

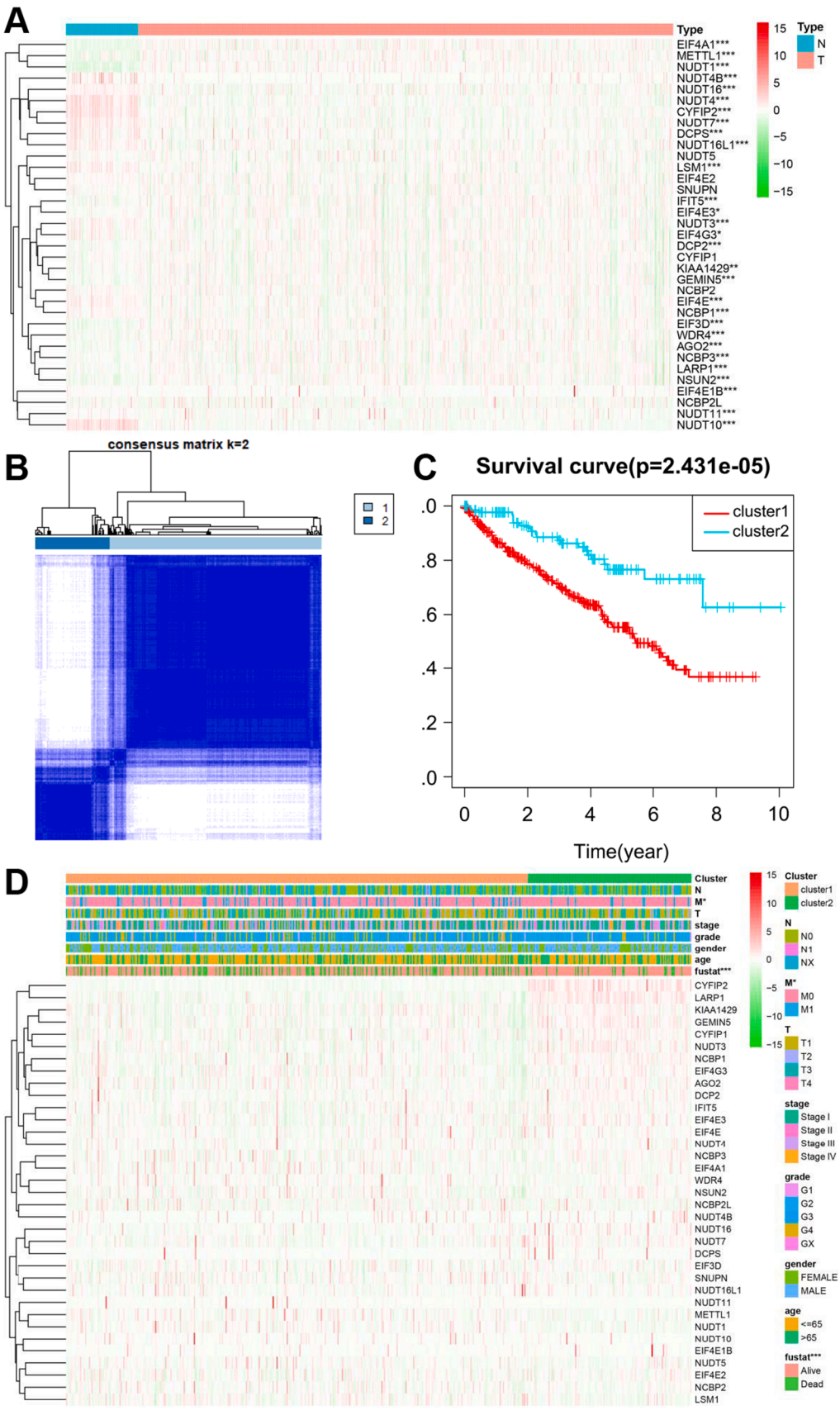


(caption on next page)

**Fig. 1.** Consensus clustering of m7G regulators. (A) Heatmap of the expression of 34 m7G RNA methylation regulators in ccRCC tissues compared. Red indicates upregulation, while green indicates downregulation. Notably, 12 genes, including METTL1 and WDR4, were significantly upregulated, while 14 genes, such as DCPS and NUDT10, were significantly downregulated ($P < 0.05$).(B) The ccRCC patients were divided into two clusters for k = 2. (C) Kaplan-Meier curves of overall survival of ccRCC patients reveals that patients in cluster 1 had significantly poorer overall survival compared to those in cluster 2 ($P < 0.001$).(D) The heatmap illustrates the associations between clinicopathological characteristics and the expression of each m7G RNA methylation regulator in the two clusters. The M stage and survival status showed significant associations with the clustering, suggesting that these m7G regulators may play a role in ccRCC progression and patient outcomes.*$P < 0.05$, **$P < 0.01$, and ***$P < 0.001$.

divided into two subgroups based on the median score of patients with ccRCC to obtain low- and high-risk groups. The overall survival curves of the two groups were drawn using the Kaplan-Meier method, and the accuracy of the RNA signature was evaluated based on the receiver operating characteristic (ROC) curves.

*Univariate and multivariate Cox regression analyses*

To determine whether the m7G-regulator-based risk score is an independent prognostic factor, univariate and multivariate Cox regression analyses were performed using the 'survival' and 'forestplot' packages. With the exception of the risk score, we investigated the effect of age (≤65 and >65 years), gender, grade, and T, N, and M stages on survival. Variables such as Mx, Tx, Nx, and unknown or ambiguous values were excluded. Factors with a $p$-value<0.05 in univariate analysis were inputted in multivariate Cox regression, after which factors with a $p$-value<0.05 and a hazard ratio [HR] >1 were considered independent prognostic factors.

*Tumor microenvironment and tumor-infiltrating immune cells*

The ESTIMATE algorithm (version 4.1.0) [25] of R was used to determine the proportion of immune-stromal components in the tumor microenvironment (TME) of the normal and tumor groups. The results are presented as the immune, stromal, and ESTIMATE scores. CIBERSORT, an algorithm reported by Newman et al. [26], was used to quantify the 22 infiltrating immune cells based on normalized gene expression profiles, which was verified by fluorescence-activated cell sorting. The 22 different immune cells included memory B cells, naive B cells, plasma cells, resting/activated natural killer (NK) cells, and seven different T cell types (CD8+ T cells, regulatory T cells [Tregs], resting/activated memory CD4+T cells, follicular helper T cells, naïve CD4+ T cells, and gamma delta T cells) [27]. Each sample was given a proportion of immune cells equal to the sum of all estimated values. Based on ccRCC gene expression data, the CIBERSORT algorithm was used to determine the relative proportions of these immune cells in the TME.

*Prediction of the effect of immunotherapy and chemotherapy*

The 'ggstatsplot' package was used to investigate the relationship between gene expression and efficacy of common immune checkpoint inhibitors. Based on the TCGA-KIRC dataset, the half-maximal inhibitory concentration values of common chemotherapeutics were calculated using the 'pRRophetic' package [28] to determine the sensitivity of the target genes to chemotherapy.

*Tissue microarray analysis*

ccRCC tissue microarrays were purchased from Guilin Fanpu Biotechnology Co., Ltd. (Guilin, China) and included 46 ccRCC samples from patients and 46 adjacent normal tissues as controls. METTL1 antibody was purchased from Invitrogen Inc. (1:1000; PA5-80810; UK). The secondary antibody used was a biotinylated goat anti-rabbit IgG antibody (Abcam, UK). To assess the expression level of METTL1, the histochemistry score (H-score) was calculated using the following formula: H-score = summation (i × pi), where i is the intensity score and pi is the percentage of cells with that intensity. Intensity scores were categorized as 0 (absent), 1 (weak), 2 (moderate), or 3 (strong).

*Statistical analysis*

*t*-test or one-way analysis of variance was used to analyze continuous variables, and chi-square test or Fisher's exact test was used for categorical variables. Gene signatures were evaluated using univariate and multivariate Cox regression analyses. Statistical analyses were performed using R software (version 4.1.0). Statistical significance for all analyses was set at $P<0.05$.

## Results

*Differentially expressed and prognostic-related genes in ccRCC*

Among the 34 m7G regulator genes, 26 were significantly differentially expressed ($P<0.05$). Compared with those in the normal controls, 12 genes, namely METTL1, WDR4, NSUN2, DCP2, NUDT1, AGO2, GEMIN5, LARP1, NCBP3, EIF3D, EIF4A1, and IFIT5, were significantly upregulated. whereas 14 genes, namely DCPS, NUDT10, NUDT11, NUDT16, NUDT16L1, NUDT3, NUDT4, NUDT4B, NUDT7, CYFIP2, EIF4E, EIF4E1B, NCBP1, and LSM1, were significantly downregulated in patients with ccRCC (Fig. 1A).

*Consensus clustering of m7G regulators identified two subgroups of ccRCC with different clinicopathological characteristics and prognosis*

The optimal value of k was determined to be 3 according to the CDF curve (Fig. S1). Although k = 3 was initially determined optimal, we chose k = 2 for further analysis due to the large overlap between groups and the small sample size in one group when using k = 3. This decision prioritized robust clustering with adequate sample sizes in each group. Based on the consistent clustering analysis of m7G regulators in ccRCC, two subgroups were identified (Fig. 1B). Kaplan-Meier survival analysis indicated that cluster 1 had a significantly poorer outcome than cluster 2 ($P<0.001$; Fig. 1C). Furthermore, the distribution of clinicopathological characteristics in clusters 1 and 2 is illustrated using a heatmap. Integration of the clustering data with clinical characteristics revealed that both M stage and survival status were significantly associated with the clustering (Fig. 1D). Based on these results, these clusters of lesions are closely associated with ccRCC.

*Construction and verification of a LASSO prognostic risk model*

*Cox regression analysis and establishment of prognostic signatures*

Univariate Cox regression analysis indicated that eight genes were significantly associated with poor prognosis in ccRCC: METTL1(HR = 1.107; 95 % confidence interval [CI] = 1.060–1.157), WDR4 (HR = 1.173, 95 % CI = 1.046–1.316), NSUN2 (HR = 1.080; 95 % CI = 1.028–1.135), NUDT11 (HR = 1.362; 95 % CI = 1.248–1.487), NUDT5 (HR = 1.077; 95 % CI = 1.043–1.113), NCBP2 (HR = 1.055; 95 % CI = 1.011–1.099), EIF4A1 (HR = 1.135; 95 % CI = 1.062–1.213), and LSM1 (HR = 1.091; 95 % CI = 1.022–1.166). Meanwhile, 11 genes were negatively associated with ccRCC progression: NUDT16 (HR = 0.949; 95 % CI = 0.907–0.993), NUDT3 (HR = 0.780; 95 % CI = 0.633–0.962), NUDT4 (HR = 0.870; 95 % CI = 0.789–0.959), NUDT7 (HR = 0.646; 95 % CI = 0.527–0.791), CYFIP1 (HR = 0.920; 95 % CI = 0.886–0.955), CYFIP2 (HR = 0.943; 95 % CI = 0.924–0.963), EIF4E (HR = 0.674; 95 %

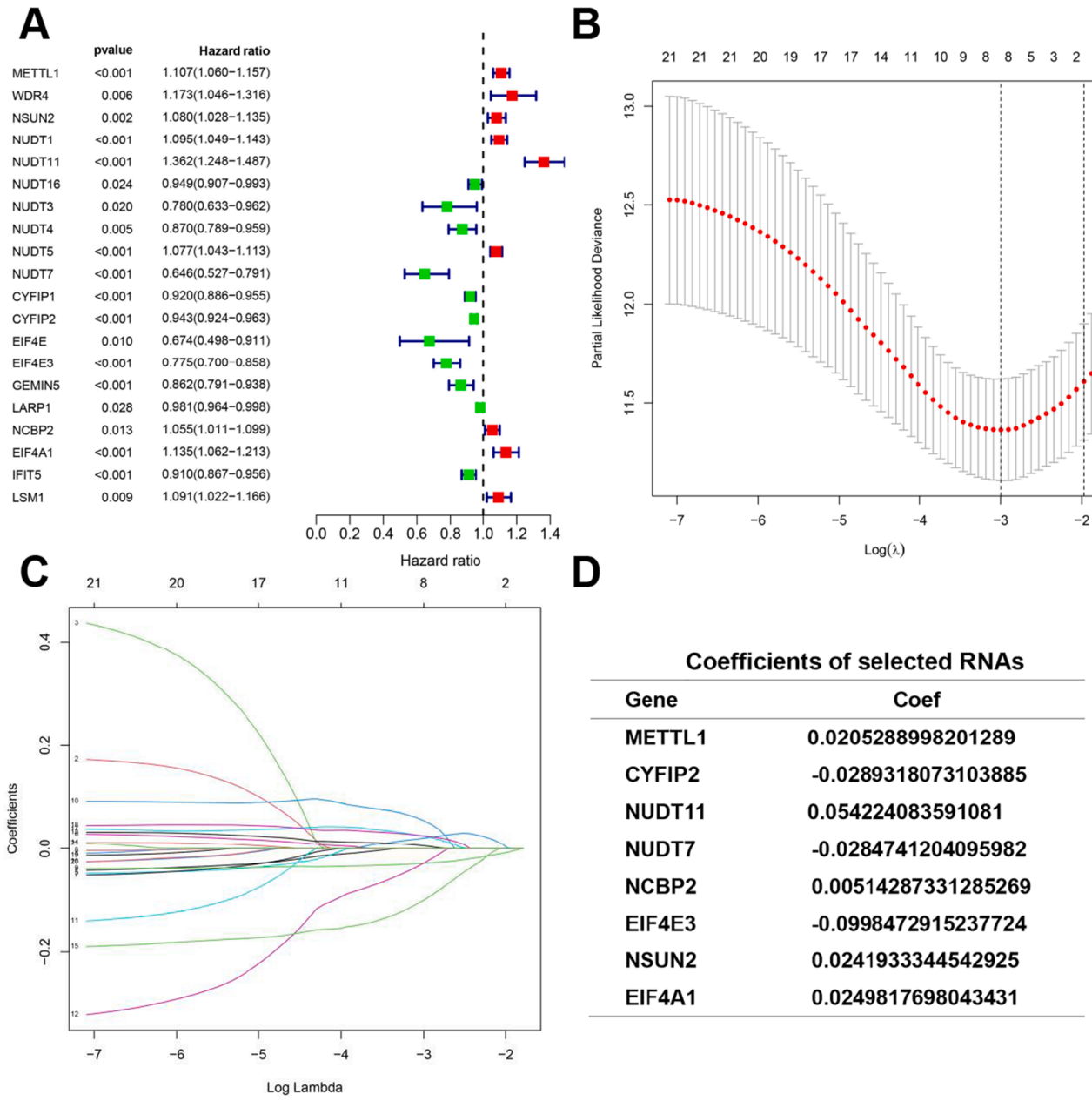


**Fig. 2.** Identification of m7G RNA methylation regulators associated with prognosis in ccRCC. A) Univariate Cox regression results showing the hazard ratios and 95 % confidence intervals for each m7G RNA methylation regulator. Eight genes, including METTL1 and WDR4, were significantly associated with poor prognosis (HR > 1, P < 0.05), while 11 genes, such as NUDT16 and NUDT3, were negatively associated with ccRCC progression (HR < 1, P < 0.05). (B-C) The least absolute shrinkage and selection operator (LASSO) regression was used to select the most prognostic-related genes. (D) The coefficients of selected RNAs identified eight genes (METTL1, CYFIP2, NUDT11, NUDT7, NCBP2, EIF4E3, NSUN2, and EIF4A1) as key predictors in the prognostic model.

CI = 0.498–0.911), EIF4E3 (HR = 0.775; 95 % CI = 0.700–0.858), GEMIN5 (HR = 0.862; 95 % CI = 0.791–0.938), LARP1 (HR = 0.981; 95 % CI = 0.964–0.998), and IFIT5 (HR = 0.910; 95 % CI = 0.867–0.956) (Fig. 2A). Prognosis-related genes were selected using LASSO Cox regression analysis (Fig. 2B-C). Eight genes, METTL1, CYFIP2, NUDT11, NUDT7, NCBP2, EIF4E3, NSUN2, and EIF4A1, were determined to be predictor variables with nonzero coefficients in the LASSO regression model (Fig. 2D).

*Validation of the diagnostic and prognostic signature for ccRCC patients*

To construct a prognostic model of ccRCC, patients were randomly divided into training and test sets (1:1 ratio). The Kaplan-Meier curves indicated that the overall survival rate of the high-risk group was significantly lower than that of the low-risk group ($P$<0.001; Fig. 3A-B). Moreover, the time-ROC curves and area under the curve (AUC) values for the prognostic signature showed significant prognostic value for KIRC patients in the training set (1-year AUC = 0.748, 3-year AUC = 0.742, 5-year AUC = 0.776; risk AUC = 0.766, age AUC = 0.594, grade AUC = 0.626, stage AUC = 0.685; Fig. 3C-D) and test set (1-year AUC = 0.722, 3-year AUC = 0.672, 5-year AUC = 0.693; risk AUC = 0.693, age AUC = 0.607, grade AUC = 0.710, stage AUC = 0.754; Fig. 3E-F). Additionally, the scatter and risk score distribution plots demonstrated a correlation between survival status and risk scores in the training (Fig. S2A-B) and test sets (Fig. S2D-E). The heat maps also indicated consistent expression of the eight m7G prognosis-related genes in both datasets (Fig. S2C, S2F).

Factors such as age, sex, stage status, grade, TNM classification, subgrouping, and immune score were integrated into the prognostic

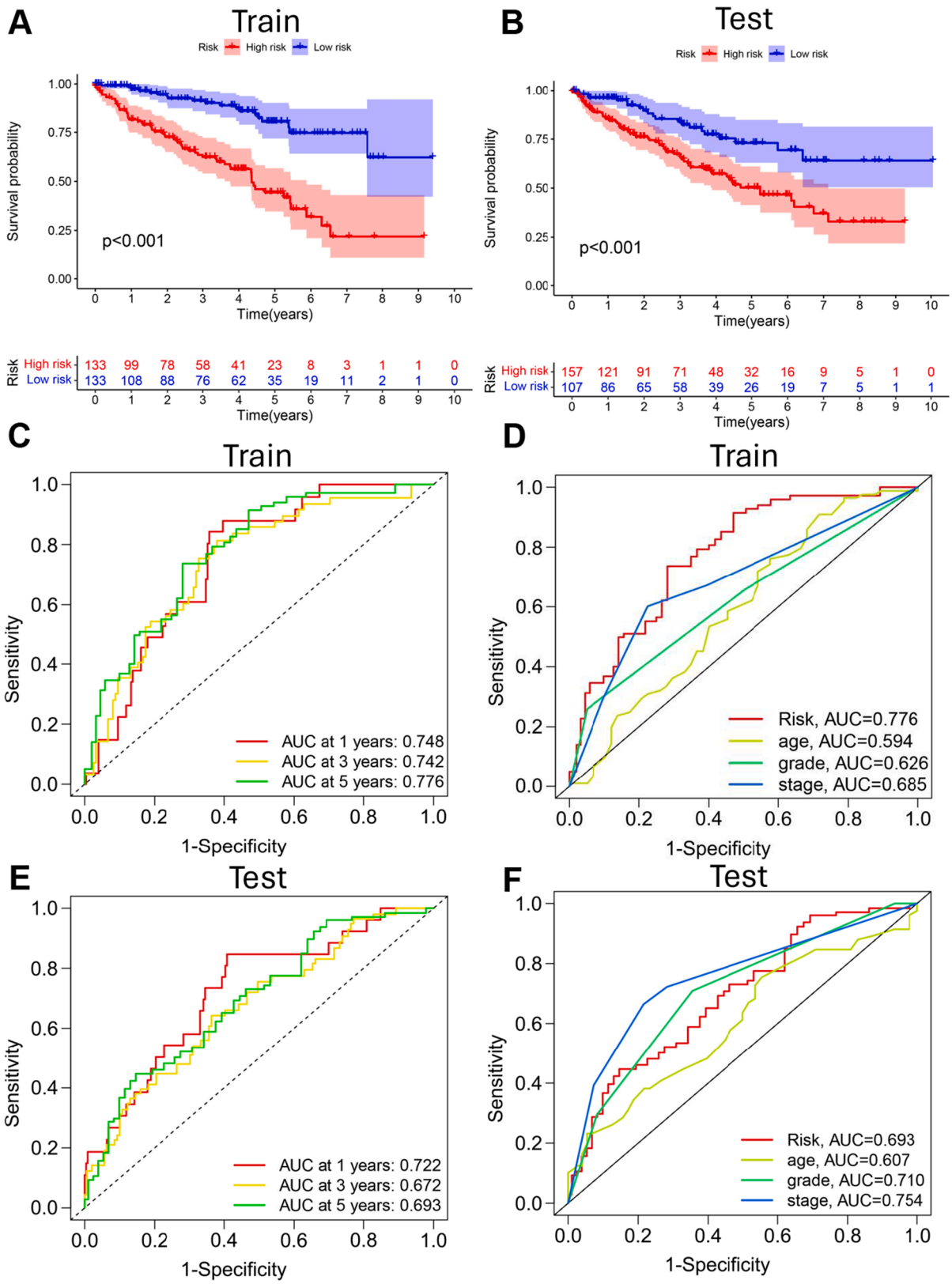


**Fig. 3.** Evaluates the prognostic risk model for overall survival in ccRCC patients. (A-B) The Kaplan-Meier curves of overall survival for patients in high- and low-risk groups in the training and test sets, respectively. In both sets, patients in the high-risk group demonstrated significantly poorer overall survival ($P < 0.001$). (C, E) Receiver operating characteristic (ROC) curves and their AUC value for 1, 3, and 5year survival predictions in the training and test sets. The model showed good predictive performance, with AUC values ranging from 0.672 to 0.776 across different timepoints and datasets. (D, F) The ROC curves for prognostic risk score against other clinicopathologic characteristics in the training and test sets. The risk score showed higher AUC values (0.766 in the training set and 0.693 in the test set) compared to age, grade, and stage, indicating its superior predictive power for patient outcomes.

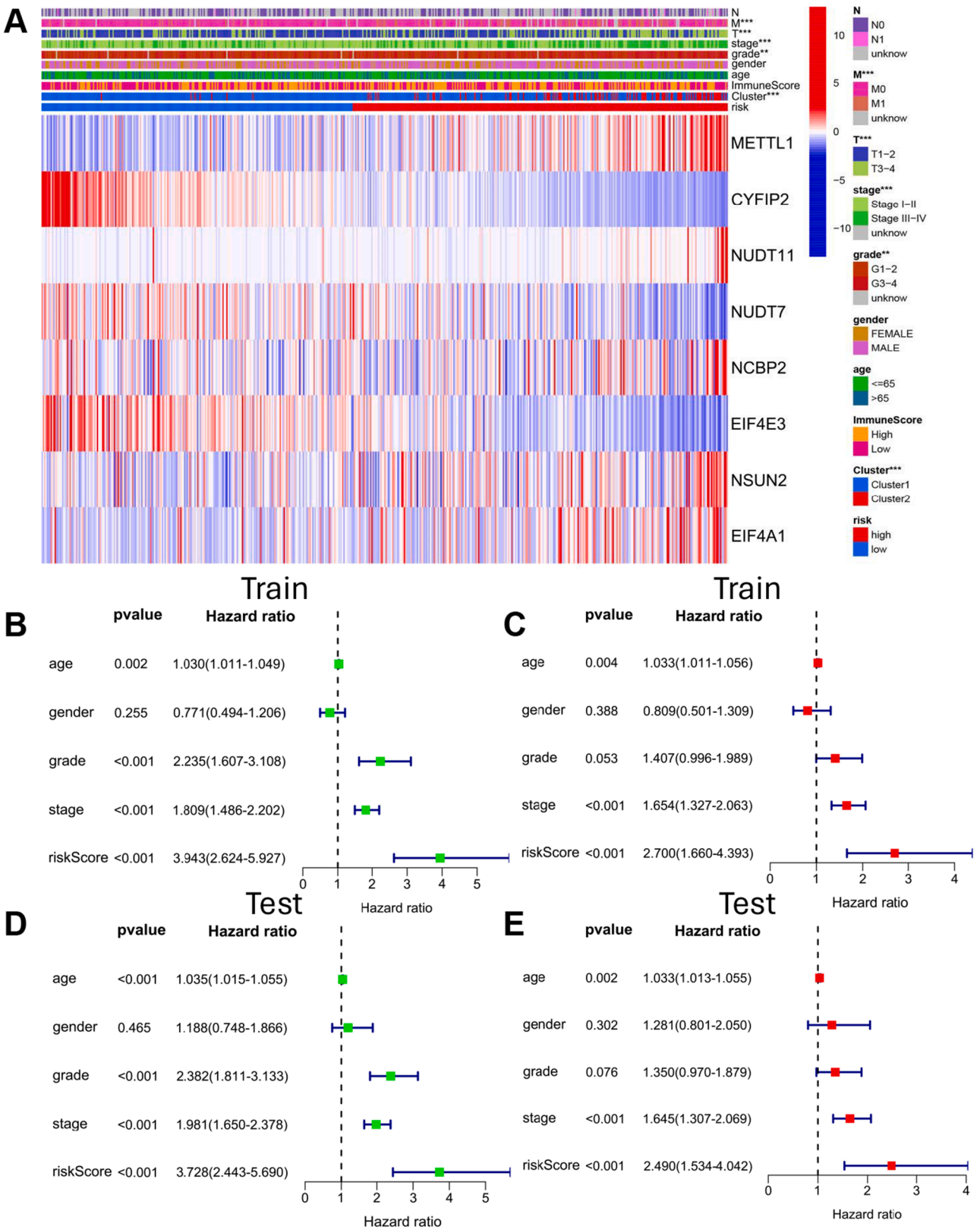


**Fig. 4.** Assesses the prognostic value of the m7G-related RNAs prognostic risk signature in ccRCC patients. (A) The heatmap showing associations between the expression of the eight m7G-related RNAs in the high- and low-risk groups, clinicopathological features, immune score, and clusters. This visualization reveals distinct expression patterns between the risk groups and their correlation with clinical characteristics. (B) Univariate and (C) multivariate Cox analyses of the risk score model with clinicopathological features (including age, gender, grade, and stage) in the training set. Similarly, (D) Univariate and (E) multivariate Cox analyses show these analyses in the test set. In both sets, the risk score remained an independent prognostic factor after adjusting for other clinical variables, underscoring its robust predictive power.

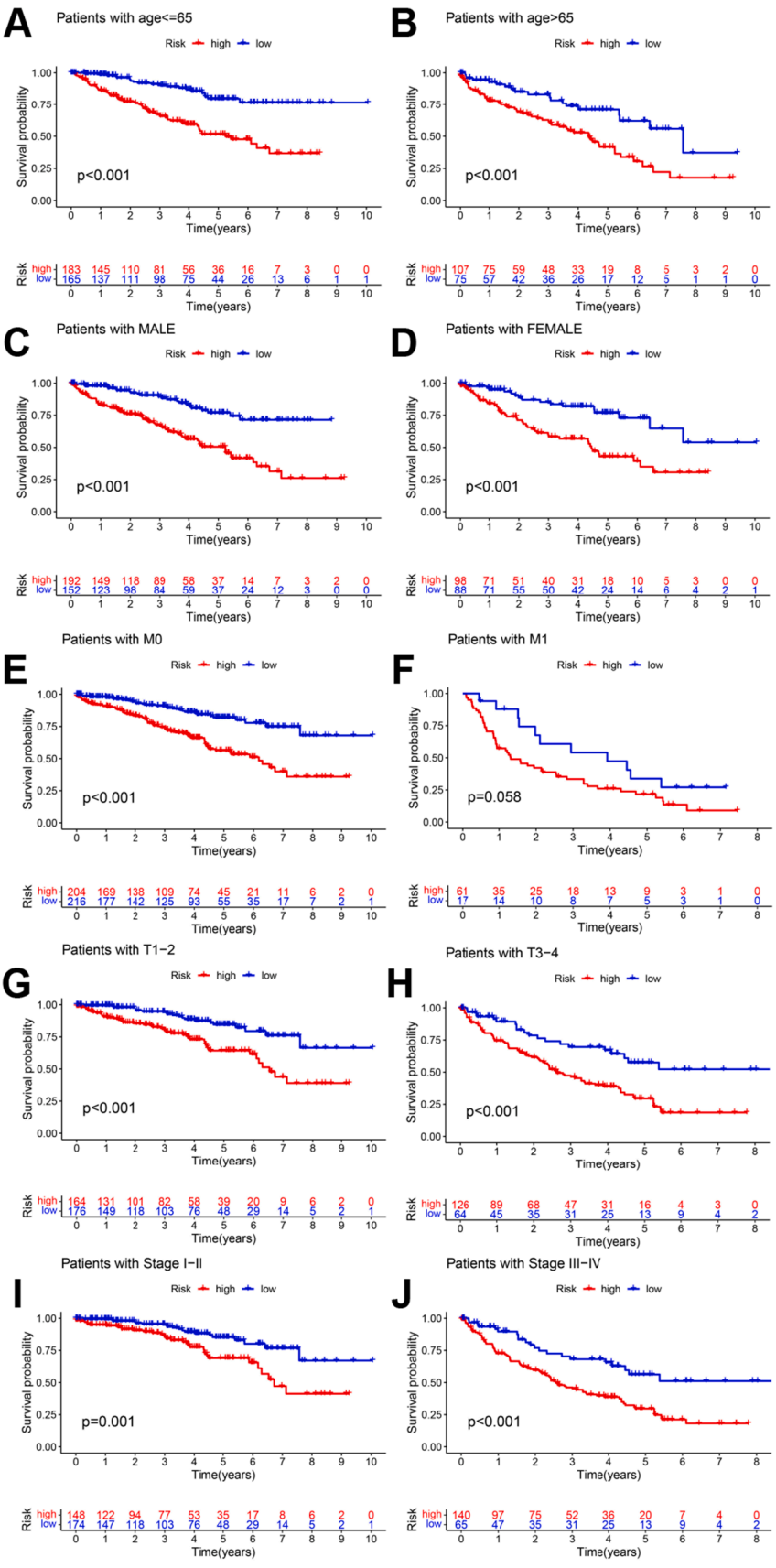


(caption on next page)

**Fig. 5.** Survival outcomes of high- and low-risk score subgroups among ccRCC patients, stratified by various clinicopathological features and METTL1 expression in ccRCC tissues. (A, B) Kaplan-Meier survival curves for patients stratified by age (>60 years vs. ≤60 years), demonstrating that the risk score maintains its prognostic value across age groups. (C, D) The survival differences between risk groups when stratified by gender. (E, F) The survival curves stratified by M stage. (G, H) The survival curves stratified by T stage. (I, J) The survival outcomes for TNM stages (stage I–II vs. stage III–IV). Across all these clinicopathological subgroups, patients in the high-risk group consistently showed poorer survival outcomes compared to those in the low-risk group, highlighting the robustness of the risk score as a prognostic indicator.

models. These models revealed significant correlations between the high-/low-risk groups and variables such as M status, T status, stage, grade, and cluster (Fig. 4A). Whether the risk scores and various clinicopathological characteristics were independent prognostic indicators was determined using univariate and multivariate Cox regression analyses. The results showed that overall survival was positively correlated with the risk score, age, and staging status ($P<0.05$; Fig. 4B-E).

Moreover, we used stratified analysis to evaluate the prognostic value of the m7G risk genes based on age (>65 years vs. ≤65 years), gender (women vs. men), grade (G1–2 vs. G3–4), M stage (M0 vs. M1), T stage (T1-2 vs. T3-4), and TNM stages (stage I-II vs. stage III-IV). Kaplan-Meier survival analysis revealed that age, stage, and risk score were significantly correlated with overall survival ($P<0.05$; Fig. 5A–J). Univariate and multivariate Cox regression analyses indicated that this risk signature was an independent prognostic indicator. These results indicate that the m7G risk score for ccRCC may serve as an independent marker of ccRCC progression.

*METTL1 predicts the ccRCC progression*

METTL1, a key prognostic-related gene, was significantly upregulated in patients with ccRCC ($P = 0.001$; Fig. 6A). A comprehensive evaluation of the m7G-related METTL1 RNA prognostic signature was conducted to confirm its predictive power for overall survival and progression-free survival (PFS). Notably, a strong association was observed between METTL1 expression and survival outcomes (Fig. 6B) and PFS (Fig. 6C); patients with elevated METTL1 expression had significantly poorer outcomes. Time-dependent ROC curves and AUC values further substantiated the high prognostic significance of METTL1 expression in the prognostic signature (1-year AUC = 0.626, 3-year AUC = 0.633, and 5-year AUC = 0.623; Fig. 6D).

The association between METTL1 expression and ccRCC progression was confirmed using tissue microarrays. The clinical characteristics of the patients are presented in Table 1. Immunohistochemistry revealed elevated METTL1 levels in patients with ccRCC (Fig. 6E-F), with an AUC of 0.823 (Fig. 6G). Survival probability assessments suggested that higher METTL1 expression was associated with poorer prognosis (Fig. 6H).

*Correlation of METTL1 expression with prognostic factors in ccRCC*

We analyzed the differences in METTL1 expression in relation to patient clinical characteristics, such as age, sex, TNM stage, and tumor grade. Our heatmap demonstrated significant associations between METTL1 expression levels and factors such as age, stage, and grade (Fig. 7A). Further exploration of the relationship of METTL1 expression with clinical features, including age (>65 vs. ≤65 years), gender (women vs. men), grade (G1-G4), and TNM stage (I-IV), as well as T (T1-T4), M (M0 vs M1), and N (N0 vs N1) stages, revealed notable disparities (Fig. 7B-H). Univariate Cox regression analysis and a clinical correlation heatmap indicated that age, stage, and tumor grade were correlated with METTL1 expression, confirming their status as independent prognostic factors (Fig. 7I).

*METTL1's role in immune cell dynamics and checkpoint expression*

To investigate the relationship of METTL1 with immune cell infiltration, we analyzed differences in the proportion of immune cells using the CIBERSORT algorithm. Fig. 8A-B show the percentages of the 22 immune cell types per sample. Our findings revealed significant variations in 10 tumor-infiltrating immune cells, namely naïve B cells, CD8+ T cells, resting and activated CD4+ memory T cells, follicular helper T cells, Tregs, monocytes, M0 macrophages, resting dendritic cells, and resting mast cells (Fig. 8C). Moreover, METTL1 expression correlated positively with Tregs, M0 macrophages, and follicular helper T cells, and negatively with follicular helper T cells and resting dendritic cells (Fig. 8D), with Tregs showing the strongest positive correlation ($R = 0.29$; $P<0.001$).

Moreover, we assessed the roles of stromal and immune cells within the immune microenvironment, focusing on the influence of METTL1 on the TME characterization in ccRCC. The analysis indicated a higher stromal score in the low METTL1 expression group, with no significant variance in the immune scores (Fig. 8E). METTL1 expression positively correlated with the expression of TMIGD2, TNFSF9, TNFRSF18, and CD70 and inversely correlated with that of other markers (Fig. 8F), which reinforces its effect on the immune environment of ccRCC.

We also explored the correlation between METTL1 expression and drug sensitivity. Elevated METTL1 levels were significantly linked to increased sensitivity to several drugs ($P<0.05$), including vinorelbine, mitomycin C, doxorubicin, etoposide, salubrinal, and pyrimethamine (Fig. S3), indicating its potential as a predictive biomarker of treatment efficacy.

## Discussion

ccRCC is one of the most lethal cancers of the genitourinary tract and is diagnosed in 70–80 % of patients with RCC [29]. Studies have reported a 2 % annual increase in the incidence of RCC worldwide over the past two decades, amounting to an average of 295,000 newly diagnosed cases of RCC and 134,000 RCC-related deaths each year [7]. Recent reports have indicated the emergence of new favorable subsets of cancers of undefined origin (CUP), including RCC-CUP, which are treated as RCC and thus contribute to its increasing incidence [30]. Additionally, several imaging technologies, such as $^{99m}$Tc-sestamibi single photon emission computed tomography/computed tomography (SPECT/CT) and Girentuximab positron emission tomography computed tomography (PET-CT) molecular imaging, are able to accurately identify RCC with smaller diameters, thereby helping guide treatment decisions, reducing unnecessary surgical risks and minimizing complications [31]. Building upon these advances in imaging technology, future studies could explore the potential of using PET-CT to detect METTL1 expression levels in ccRCC patients. This novel approach could potentially combine the spatial resolution of PET-CT with the prognostic value of METTL1 expression, offering a non-invasive method to assess ccRCC progression and prognosis. Such an integrated approach could provide clinicians with more comprehensive information for treatment planning and monitoring, potentially improving patient outcomes.

Currently, effective prognostic markers for ccRCC are lacking, owing to its highly heterogeneous nature and complicated disease processes. Thus, identification of novel biomarkers is urgently needed to predict the long-term survival of patients with the disease. Additionally, the bilayer membrane structure of exosomes makes them highly resistant to enclosed RNases and proteases, which enhances the stability of the encapsulated mRNAs, miRNAs, and functional proteins, making exosomes effective diagnostic markers. Furthermore, the cargo in tumor-derived exosomes, which contain miRNAs, may serve as biomarkers of ccRCC in the serum and urine of patients, providing valuable targets for

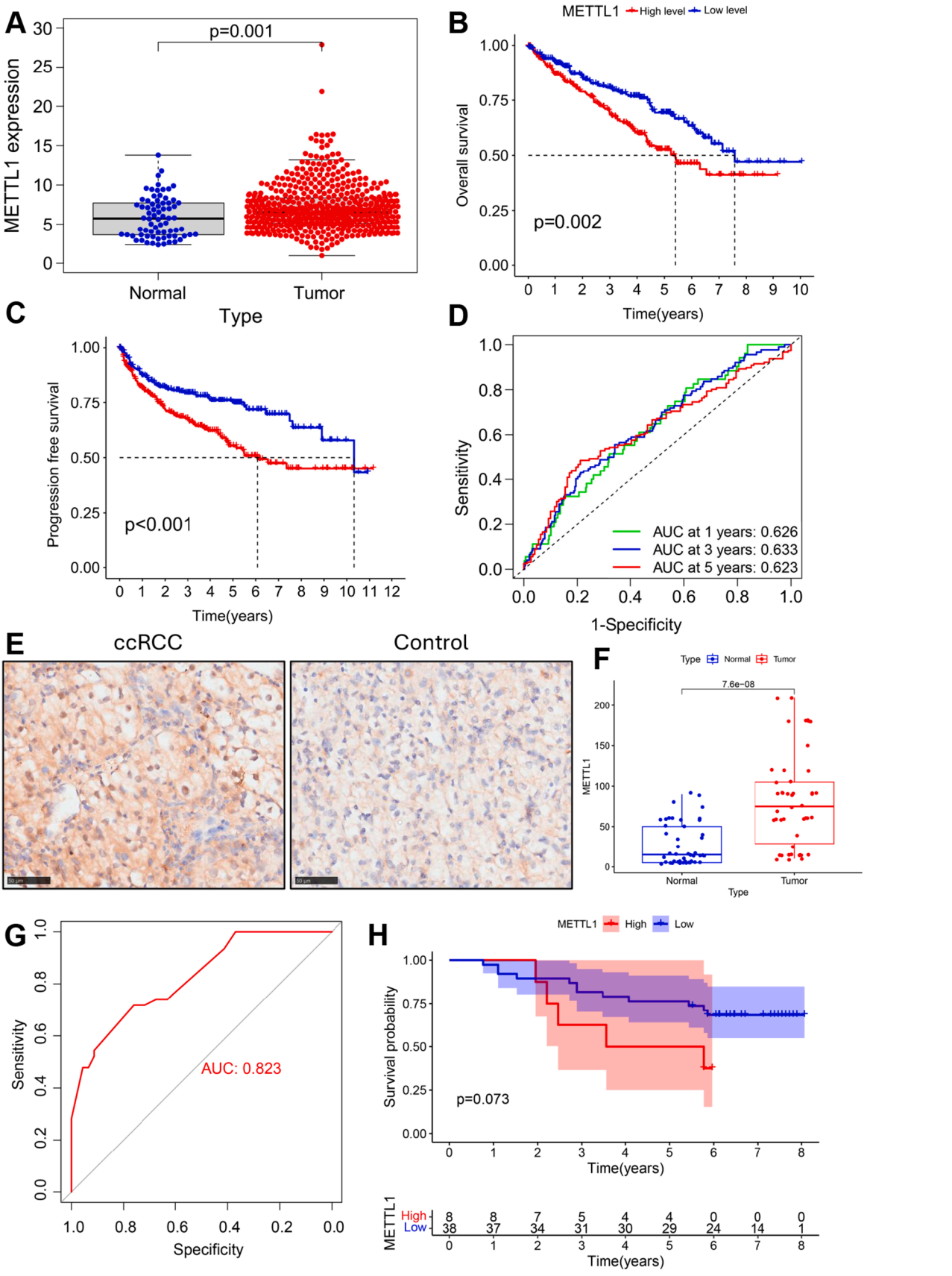


*(caption on next page)*

**Fig. 6.** The prognostic value of METTL1 in ccRCC patients. A) METTL1 expression in ccRCC (n = 537) compared to normal tissues (n = 72) in the TCGA dataset, revealing significantly higher expression in tumor tissues (P = 0.001). (B-C) The Kaplan-Meier curves illustrating overall survival and progression-free survival among high-risk and low-risk groups, stratified by METTL1 expression. Patients with high METTL1 expression consistently showed poorer survival outcomes. (D) The receiver operating characteristic (ROC) curves with corresponding AUC value for 1-, 3-, and 5-year survival predictions based on METTL1 expression in the TCGA dataset. The AUC values (0.626, 0.633, and 0.623 for 1-, 3-, and 5-year predictions, respectively) indicate moderate predictive performance. (E-F) The immunohistochemistry results of METTL1 in ccRCC compared to normal tissues and its expression in ccRCC tissue microarrays. (F) The ROC curve for METTL1 expression in ccRCC tissue microarrays, corresponding AUC value 0.823, suggesting strong diagnostic potential for METTL1. (H) The survival probability assessments of METTL1 expression in ccRCC tissue microarrays further confirming its prognostic value.

**Table 1**
Clinical and pathological characteristics of 46 paired ccRCC tumor tissues and adjacent normal tissues.

| | Tumor (n=46) | Normal (n=46) |
|---|---|---|
| Age | | |
| <60 | 25 | 25 |
| ≥60 | 21 | 21 |
| Gender | | |
| Female | 13 | 13 |
| Male | 33 | 33 |
| Tumor size | | |
| <5cm | 10 | / |
| ≥5cm | 36 | / |
| T stage | | |
| T1 | 17 | / |
| T2 | 21 | / |
| T3 | 8 | / |
| N stage | | |
| N0 | 42 | / |
| N1 | 2 | / |
| N2 | 2 | / |
| M stage | | |
| M0 | 38 | / |
| M1 | 8 | / |
| Dead | | |
| No | 29 | / |
| Yes | 17 | / |
| tumour recurrence | | |
| No | 38 | / |
| Yes | 8 | / |
| Survival time(day) | 2208.00(1302.00,2697.00) | / |
| AFP(ng/mL) | 54.30(12.30,210.00) | / |
| CEA(ng/mL) | 3.70(1.90,32.10) | / |

early detection and monitoring [32].

Recent studies have shown that RNA methylation is associated with the development of various cancer types. In a recent study, m6A has been shown to be one of the most prevalent types of mRNA modification and has been extensively studied in glioblastoma, colorectal cancer, pancreatic cancer, hepatocellular carcinoma, acute lymphoblastic leukemia, and other malignancies [33]. In contrast, m7G methylation modifications have rarely been studied. However, this modification is critical for controlling tumorigenesis, proliferation, metastasis, and tumor-associated immunity. To date, no comprehensive study has investigated the effect of m7G on ccRCC. In this study, differential analysis revealed significant differences in the expression levels of m7G RNA methylation regulators between normal and renal clear cell carcinoma tissues, suggesting that m7G RNA methylation-modified genes, such as METTL1, CYFIP2, NUDT11, NUDT7, NCBP2, EIF4E3, NSUN2, and EIF4A1, may play important roles in the development of ccRCC. Furthermore, the association between risk scores and patient characteristics indicated that gene-related regulation was involved in ccRCC differentiation and progression.

Studies have shown that METTL1 plays a critical role in m7G modification [34]. METTL1 has been shown to function in the self-renewal and differentiation of embryonic stem cells [35]; however, its role in cancer remains unclear. Several recent studies have found that tRNA m7G methyltransferase METTL1 is overexpressed in cancers and is associated with poor patient outcomes and resistance to chemotherapy, implying the potential role of METTL1 in cancer biology. Furthermore, METTL1 overexpression was found to be associated with poor prognosis and resistance to chemotherapy [36]. However, molecular insights into the role of METTL1 in ccRCC are limited. In the present study, differential analysis demonstrated that METTL1 expression in ccRCC tissues was significantly higher than that in normal tissues, which was validated using HPA. Furthermore, survival analysis showed that patients with high METTL1 expression had a shorter survival time and poor prognosis and that METTL1 was strongly associated with clinical characteristics. METTL1 overexpression has been reported to be associated with a poor prognosis in cancers such as liver cancer, intrahepatic cholangiocarcinoma (ICC), lung cancer, and colon cancer [37,38]. Collectively, these data demonstrate the potential prognostic value of METTL1 in patients with ccRCC.

Many studies have investigated the mechanism of action of METTL1 in tumors. A study reported that METTL1 promoted esophageal squamous cell carcinoma (ESCC) tumorigenesis via the RPTOR/ULK1/autophagy axis and that it may serve as a therapeutic target for ESCC [11]. METTL1 was found to contribute to head and neck squamous cell carcinoma progression through the PI3K/AKT/mTOR signaling pathway [35]. A recent study has shown that METTL1 overexpression promoted the proliferation and migration of hepatocellular carcinoma cells by activating the phosphatase and tensin homolog deleted on chromosome ten signaling pathway [39]. In the present study, the GSEA results showed significant enrichment of genes associated with oxidative phosphorylation and ribosomes in the high METTL1 expression population, suggesting that METTL1 promotes ccRCC cell proliferation, migration, and invasion through the regulation of oxidative phosphorylation and ribosome pathways. Rapidly dividing cells such as cancer cells must maintain optimal protein levels, and ribosomes, which are molecular machines that synthesize proteins, are at central to this regulation. Recent studies have established that METTL1/WDR4 play an important role in ribosome biogenesis and mRNA translation by introducing m7G modifications into rRNA and tRNA [40]. As a major component of the protein synthesis factory, tRNAs are more complex than mRNA, and their modifications can affect tRNA stability, mRNA translation, and rates of protein synthesis [41]. These studies demonstrate that abnormal tRNA expression levels and METTL1-mediated modifications of m7G tRNA could lead to cancer progression by interfering with translation and protein synthesis. Furthermore, sufficient evidence indicates that METTL1 can increase VEGFA mRNA translation by upregulating its m7G and that METTL1 can stimulate angiogenesis to accelerate cancer cell proliferation and migration in a VEGFA-dependent manner [42]. However, the physiological functions and molecular mechanisms underlying METTL1-mediated m7G tRNA modifications in ccRCC remain unclear. Hence, our study provides new insights into m7G tRNA modifications in ccRCC. Thus, drugs targeting METTL1 can achieve therapeutic effects by inhibiting ribosomal protein synthesis and selective translation of cancer-promoting mRNA to slow down or passivate the growth and proliferation of tumor cells.

Several studies have indicated that ccRCC is an immunogenic malignancy and that numerous immune cells, such as CD8+ T cells, CD4+ T cells, macrophages, natural killer cells, and myeloid-derived suppressor cells, infiltrate its TME [43]. Nonetheless, tyrosine kinase inhibitor (TKI) monotherapy remains the appropriate first-line treatment for a significant proportion of the patients who do not respond to immunotherapy. The STAR study showed no clinically significant reduction in life expectancy and treatment breaks between the drug-free interval strategy

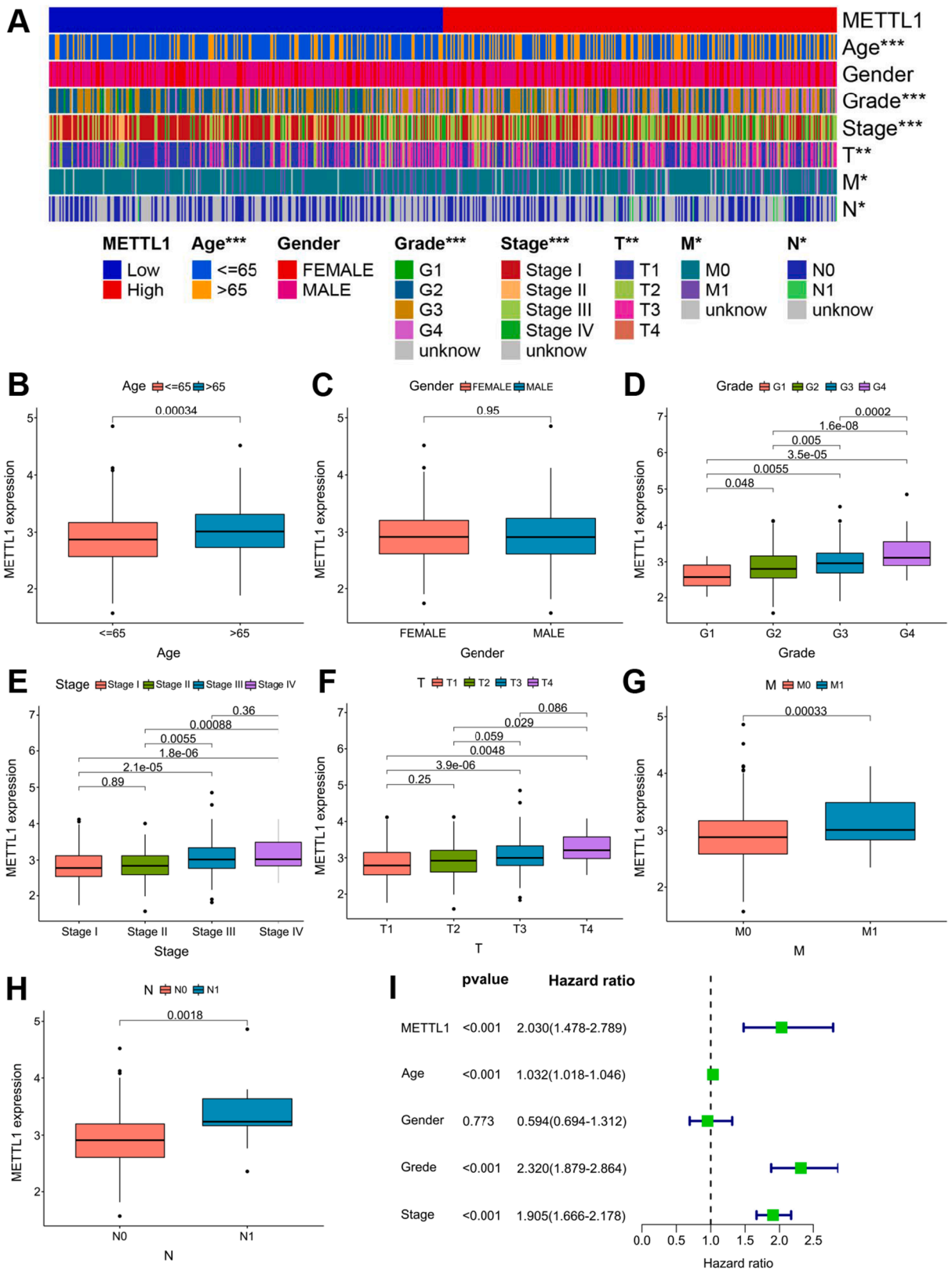


**Fig. 7.** Comprehensive analysis of METTL1 expression and its prognostic value in ccRCC A) The heatmap illustrating the associations between METTL1 expression levels and key clinicopathological characteristics. This visualization reveals distinct patterns of METTL1 expression across different patient subgroups, highlighting its potential role in ccRCC progression. (B-H) The box plots that depict the METTL1 expression in specific clinicopathological features. I) The univariate Cox regression analyses, displaying hazard ratios with 95 % confidence intervals for METTL1 expression and various clinicopathological features. This forest plot illustrates that elevated METTL1 expression, along with other factors such as advanced age, higher grade, and later stage, are associated with poorer prognosis in ccRCC patients

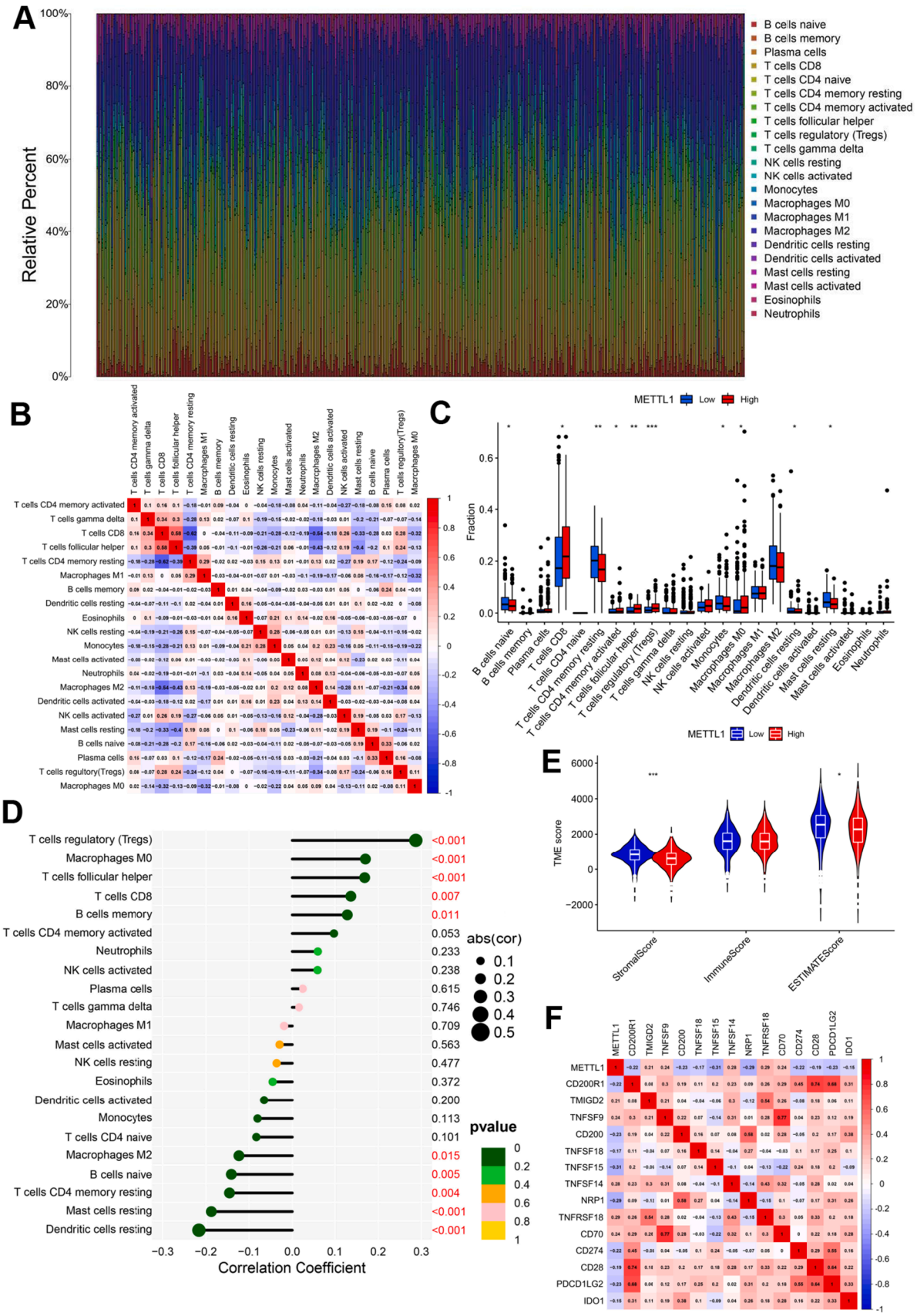


*(caption on next page)*

**Fig. 8.** METTL1 expression and its relationship with tumor-infiltrating immune cells and the tumor microenvironment in ccRCC. (A) The stacked bar chart showing the relative proportions of 22 different tumor-infiltrating immune cell (TIC) types across individual ccRCC samples. This visualization provides an overview of the immune cell composition within the tumor microenvironment, highlighting the heterogeneity among patients. (B) The correlation heatmap among the 22 TIC types. The color intensity and size of the circles indicate the strength and direction of correlations between different immune cell populations, offering insights into potential interactions within the tumor immune microenvironment (C) The box plots comparing the infiltration levels of the 22 immune cell types between high and low METTL1 expression groups. These plots reveal significant differences in immune cell compositions based on METTL1 expression levels. (D) The correlation between METTL1 expression and the infiltration levels of various immune cell types. (E) The violin plots comparing tumor microenvironment (TME) scores between high and low METTL1 expression groups. The plots depict differences in stromal scores, immune scores, and overall ESTIMATE scores, providing insights into how METTL1 expression might influence the composition of the tumor microenvironment. (F) The correlation heatmap between METTL1 expression and various immune checkpoint molecules. This visualization helps identify potential relationships between METTL1 and key regulators of the immune response in ccRCC.

and conventional continuation strategy groups, indicating that it may be an affordable and cost-effective treatment option with lifestyle benefits for patients with RCC during tyrosine kinase inhibitor therapy [44]. Some patients may not receive TKI as first-line treatment but may do so as monotherapy as second-line treatment. However, while treatment breaks in these patients are reasonable, caution should be exercised because these patients are more likely to have shorter progression-free survival than those receiving first-line TKIs. CD8+ T cell infiltration and CD4+ T cell hyperproliferation are associated with cancer severity and shortened survival in ccRCC. High CD8+ T cell proliferation rates are also associated with prolonged survival in patients with ccRCC, suggesting that the functional status of immune cells significantly affects the activity of antitumor immune cells. Failure of tumor-infiltrating lymphocytes to perform antitumor functions could be explained by the large infiltration of immunosuppressive cells such as Treg cells [45].

This study also aimed to explore the association between METTL1 expression and immune cell infiltration. Tregs were positively correlated with METTL1 expression. Therefore, we hypothesized that METTL1 promotes Treg infiltration. Studies have shown that Tregs actively participate in the inhibition of abnormal immune responses to autoantigens and play a leading role in impairing antitumor responses and promoting tumorigenesis [46]. The high infiltration rate of Tregs in the TME is associated with poor patient prognosis in various malignant tumors, such as non-small cell lung cancer, ovarian cancer, glioblastoma multiforme, and pancreatic ductal adenocarcinoma [47–50]. Tregs can mediate immunosuppression by secreting immunosuppressive cytokines and expressing cell surface inhibitory receptors to inhibit antigen-presenting cell maturation, deplete IL-2, and regulate effector T cell function, among others [51]. Therefore, METTL1 overexpression may promote immune escape in ccRCC. Subsequently, we conducted immune checkpoint studies, which demonstrated that METTL1 expression positively correlated with the expression of TMIGD2, TNFSF9, TNFSF9, TNFRSF18, and CD70, suggesting that immune checkpoint inhibitors along with inhibition of METTL1 expression in ccRCC patients may improve better therapeutic outcomes. Nonetheless, numerous studies demonstrated that genes in the PI3K-Akt pathway, often dysregulated in ccRCC, are linked to patient prognosis and may serve as potential therapeutic targets [52,53]. Their findings regarding IL2RG, EFNA3, and MTCP1 as prognostic markers highlight the complex interplay between signaling pathways, immune responses, and clinical outcomes in ccRCC [54]. These results confirm that dysfunction in the immune microenvironment is crucial for ccRCC progression and could serve as a potential target for immunotherapy.

Our results suggest that patients with elevated METTL1 expression have significantly worse outcomes and higher clinical and pathological stages. Patients with low METTL1 expression tended to be in the early stages of the tumor, which could help in early ccRCC prediction. Immune cell infiltration analysis showed that METTL1 expression was associated with the infiltration of multiple immune cells. This suggests that METTL1 is involved in regulating the expression and function of many immune cells, thereby affecting tumor progression. Thus, targeting METTL1 may improve the immune microenvironment of ccRCC, thereby improving tumor treatment efficacy. Drug sensitivity analysis suggested that METTL1 could be used as a biomarker to predict the efficacy of vinorelbine, mitomycin C, doxorubicin, etoposide, salubrinal, and pyrimethamine in ccRCC. This could assist clinicians in evaluating reasonable medication options.

Nonetheless, this study has several limitations. First, our analysis was based on retrospective data from TCGA database, which may introduce potential biases. Although our tissue microarray validation provided important biological confirmation, future studies should validate these findings in larger prospective cohorts to ensure generalizability and clinical applicability. Moreover, the potential mechanisms by which METTL1 contributes to ccRCC development have not been fully elucidated. Based on previous studies, several hypotheses of METTL1 biological function that may be related to ccRCC progression have been posited. METTL1-catalyzed m7G modification can stabilize certain mRNAs and enhance their translation efficiency, possibly leading to the upregulation of oncogenes and cell cycle regulators that drive proliferation and invasion. Additionally, METTL1 promotes ribosome biogenesis and global protein synthesis, which may be particularly important for the rapid growth of cancer cells. Furthermore, the study found that METTL1 expression positively correlated with the infiltration of immunosuppressive Tregs into the ccRCC TME. This suggests that METTL1 facilitates immune evasion, allowing tumor cells to evade antitumor immune responses. Therefore, future studies should use *in vitro* and *in vivo* models to investigate the effects of METTL1-mediated m7G modifications on specific oncogenic pathways in ccRCC.

## Conclusions

Our study provides novel insights into the role of m7G RNA methylation regulators, particularly METTL1, in ccRCC. We systematically revealed the expression patterns, potential functions, and prognostic values of these regulators, with a specific focus on the critical role of METTL1 in shaping the tumor immune microenvironment.

Notably, this study is the first to demonstrate that METTL1 expression was highly correlated with the clinicopathological features of ccRCC and could serve as an independent prognostic indicator. Our findings suggest that METTL1 with CYFIP2, NUDT11, NUDT7, NCBP2, EIF4E3, NSUN2, and EIF4A1 may function as potential biomarkers for ccRCC diagnosis, prognosis, and treatment response prediction.

Furthermore, our analysis of the association between METTL1 and infiltration of immune cells, especially Tregs, provides new perspectives on how m7G methylation influences tumor immunity in ccRCC. This opens up possibilities for the development of novel immunotherapeutic strategies targeting the METTL1-mediated m7G pathway.

Our study not only advances our understanding of m7G-related gene pathogenesis in ccRCC, but also provides a foundation for developing novel diagnostic, prognostic, and therapeutic approaches targeting this pathway. Our findings may ultimately contribute to improving the outcomes of patients with ccRCC through personalized treatment strategies.

## CRediT authorship contribution statement

**Yi Liu:** Conceptualization. **Yanji Zhan:** Data curation. **Jiao Liu:** Formal analysis. **Zhengze Shen:** Formal analysis. **Yudong Hu:** Formal analysis. **Ling Zhong:** Software. **Yuan Yu:** Software. **Bin Tang:** Writing – original draft. **Jing Guo:** Writing – review & editing.

## Declaration of competing interest

The authors declared that they have no competing interests.

### *Abbreviations*

Area under the curve (AUC), 7-methylguanosine (m7G), clear cell renal cell carcinoma (ccRCC), Principal Component Analysis (PCA), Transfer RNAs (tRNA), progression-free survival (PFS), Gene Ontology (GO), Kyoto Encyclopedia of Genes and Genomes (KEGG), least absolute shrinkage and selection operator (LASSO), overall survival (OS), receiver operating characteristic (ROC), regulatory T cells (Tregs), renal cell carcinoma (RCC), The Cancer Genome Atlas (TCGA), tumor microenvironment (TME).

### *Ethics approval and consent to participate*

TCGA Ethics and Policies were originally published by the National Cancer Institute: https://www.cancer.gov/ccg/research/genome-sequencing/tcga/history/ethics-policies. The human ccRCC tissue chip was obtained from Guilin Fanpu Biotechnology Co., Ltd. (Guilin, China). All samples were obtained with the informed consent of the patients, and the study was approved by the Ethics Committee of Chongqing University Cancer Hospital, Chongqing University and Guilin Fanpu Biotechnology Co., Ltd. (Fanpu [2018] No. 23).

### *Consent for publication*

Not applicable.

### *Availability of data and materials*

We evaluated publicly available datasets found in the Cancer Genome Atlas (TCGA) database.

### *Acknowledgements*

The Cancer Genome Atlas (TCGA) database was a critical component of this study. We sincerely thank the platform and the authors for their contributions.

### *Funding*

This work was supported by the Chongqing Science and Technology Commission (Grant No. CSTB2022NSCQ0322), Chongqing Science and Health Joint Medical Research Project (Grant No. 2022MSXM047). The funders had no role in study design, data collection and analysis, decision to publish, or preparation of the manuscript.

### *Authors' contributions*

YL and JG designed the research, JL and ZS analyzed the data, YZ and YH performed bioinformatics, LZ and YY performed the statistical analyses. BT and JG draft the manuscript. All authors read and approved the final manuscript.

## Supplementary materials

Supplementary material associated with this article can be found, in the online version, at doi:10.1016/j.tranon.2024.102202.

## References

[1] KD Miller, L Nogueira, AB Mariotto, JH Rowland, KR Yabroff, CM Alfano, et al., Cancer treatment and survivorship statistics, 2019, CA A Cancer J. Clin. 69 (2019) 363–385.
[2] Z Sun, C Jing, C Xiao, T Li, Y. Wang, Prognostic risk signature based on the expression of three m6A RNA methylation regulatory genes in kidney renal papillary cell carcinoma, Aging 12 (2020) 22078–22094.
[3] RL Siegel, KD Miller, A. Jemal, Cancer statistics, 2017, CA Cancer J. Clin. 67 (2017) 7–30.
[4] H Aweys, D Lewis, M Sheriff, RD Rabbani, P Lapitan, E Sanchez, et al., Renal cell cancer – insights in drug resistance mechanisms, Anticancer Res. 43 (2023) 4781–4792.
[5] T Xu, S Gao, H Ruan, J Liu, Y Liu, D Liu, et al., METTL14 acts as a potential regulator of tumor immune and progression in clear cell renal cell carcinoma, Front. Genet. 12 (2021) 609174.
[6] Q. Zeng, Bioinformatic identification of renal cell carcinoma microenvironment-associated biomarkers with therapeutic and prognostic value, Life Sci. 8 (2020).
[7] W Deng, G Wang, H Deng, Y Yan, K Zhu, R Chen, et al., The role of critical N6-methyladenosine-related long non-coding RNAs and their correlations with immune checkpoints in renal clear cell carcinoma, IJGM 14 (2021) 9773–9787.
[8] KE Sloan, AS Warda, S Sharma, K-D Entian, DLJ Lafontaine, MT. Bohnsack, Tuning the ribosome: The influence of rRNA modification on eukaryotic ribosome biogenesis and function, RNa Biol. 14 (2017) 1138–1152.
[9] A Ramanathan, GB Robb, S-H. Chan, mRNA capping: biological functions and applications, Nucleic. Acids. Res. 44 (2016) 7511–7526.
[10] C. Tomikawa, 7-methylguanosine modifications in transfer RNA (tRNA), Int. J. Mol. Sci. 19 (2018) 4080.
[11] H Han, C Yang, J Ma, S Zhang, S Zheng, R Ling, et al., N7-methylguanosine tRNA modification promotes esophageal squamous cell carcinoma tumorigenesis via the RPTOR/ULK1/autophagy axis, Nat. Commun. 13 (2022) 1478.
[12] Z Chen, W Zhu, S Zhu, K Sun, J Liao, H Liu, et al., METTL1 promotes hepatocarcinogenesis via m7 G tRNA modification-dependent translation control, Clin. Transl. Med. 11 (2021) e661.
[13] J Ma, H Han, Y Huang, C Yang, S Zheng, T Cai, et al., METTL1/WDR4-mediated m7G tRNA modifications and m7G codon usage promote mRNA translation and lung cancer progression, Mol. Ther. 29 (2021) 3422–3435.
[14] R García-Vílchez, AM Añazco-Guenkova, S Dietmann, J López, V Morón-Calvente, S D'Ambrosi, et al., METTL1 promotes tumorigenesis through tRNA-derived fragment biogenesis in prostate cancer, Mol. Cancer 22 (2023) 119.
[15] D Du, M Zhou, C Ju, J Yin, C Wang, X Xu, et al., METTL1-mediated tRNA m7G methylation and translational dysfunction restricts breast cancer tumorigenesis by fueling cell cycle blockade, J. Exp. Clin. Cancer Res. 43 (2024) 154.
[16] P Xia, H Zhang, K Xu, X Jiang, M Gao, G Wang, et al., MYC-targeted WDR4 promotes proliferation, metastasis, and sorafenib resistance by inducing CCNB1 translation in hepatocellular carcinoma, Cell Death. Dis. 12 (2021) 691.
[17] EA Orellana, Q Liu, E Yankova, M Pirouz, E De Braekeleer, W Zhang, et al., METTL1-mediated m7G modification of Arg-TCT tRNA drives oncogenic transformation, Mol. Cell 81 (2021) 3323–3338, e14.
[18] D Yan, L Tu, H Yuan, J Fang, L Cheng, X Zheng, et al., WBSCR22 confers oxaliplatin resistance in human colorectal cancer, Sci. Rep. 7 (2017) 15443.
[19] J Liu, T Lichtenberg, KA Hoadley, LM Poisson, AJ Lazar, AD Cherniack, et al., An integrated TCGA pan-cancer clinical data resource to drive high-quality survival outcome analytics, Cell 173 (2018) 400–416, e11.
[20] L Bukavina, K Bensalah, F Bray, M Carlo, B Challacombe, JA Karam, et al., Epidemiology of renal cell carcinoma: 2022 update, Eur. Urol. 82 (2022) 529–542.
[21] MD Wilkerson, DN. Hayes, ConsensusClusterPlus: a class discovery tool with confidence assessments and item tracking, Bioinformatics. 26 (2010) 1572–1573.
[22] R. Tibshirani, Regression shrinkage and selection via the lasso, J. R. Stat. Soc. Ser. B: Stat. Methodol. 58 (1996) 267–288.
[23] J Bai, JH Huang, CPE Price, JM Schauer, LA Suh, R Harmon, et al., Prognostic factors for polyp recurrence in chronic rhinosinusitis with nasal polyps, J. Allergy Clin. Immunol. 150 (2022), 352-361.e7.
[24] S Engebretsen, J. Bohlin, Statistical predictions with glmnet, Clin Epigenet 11 (2019) 123.
[25] K Yoshihara, M Shahmoradgoli, E Martínez, R Vegesna, H Kim, W Torres-Garcia, et al., Inferring tumour purity and stromal and immune cell admixture from expression data, Nat. Commun. 4 (2013) 2612.
[26] AM Newman, CL Liu, MR Green, AJ Gentles, W Feng, Y Xu, et al., Robust enumeration of cell subsets from tissue expression profiles, Nat. Methods 12 (2015) 453–457.
[27] Zhong J, Liu Z, Cai C, Duan X, Deng T, Zeng G. m6A modification patterns and tumor immune landscape in clear cell renal carcinoma. Open access.:12.
[28] P Geeleher, N Cox, RS. Huang, pRRophetic: An R Package for Prediction of Clinical Chemotherapeutic Response from Tumor Gene Expression Levels, PLoS. One 9 (2014) 3.
[29] L Zhang, Z Su, F Hong, L Wang, Identification of a methylation-regulating genes prognostic signature to predict the prognosis and aid immunotherapy of clear cell renal cell carcinoma, Front. Cell Dev. Biol. 10 (2022) 832803.
[30] E Rassy, et al., New rising entities in cancer of unknown primary: Is there a real therapeutic benefit? Crit. Rev. Oncol. Hematol. 147 (2020 Mar) 102882.
[31] OS Tataru, M Marchioni, F Crocetto, B Barone, G Lucarelli, F Del Giudice, et al., Molecular imaging diagnosis of renal cancer using 99mTc-Sestamibi SPECT/CT and Girentuximab PET-CT-current evidence and future development of novel techniques, Diagnostics 13 (2023) 593.
[32] S Boussios, P Devo, ICA Goodall, K Sirlantzis, A Ghose, SD Shinde, et al., Exosomes in the diagnosis and treatment of renal cell cancer, Int. J. Mol. Sci. 24 (2023) 14356.
[33] J Li, Z Zuo, S Lai, Z Zheng, B Liu, Y Wei, et al., Differential analysis of RNA methylation regulators in gastric cancer based on TCGA data set and construction of a prognostic model, J. Gastrointest. Oncol. 12 (2021) 1384–1397.

[34] K Boulias, EL. Greer, Put the pedal to the METTL1: adding internal m7G increases mRNA translation efficiency and augments miRNA processing, Mol. Cell 74 (2019) 1105–1107.
[35] J Chen, K Li, J Chen, X Wang, R Ling, M Cheng, et al., Aberrant translation regulated by METTL1/WDR4-mediated tRNA N7-methylguanosine modification drives head and neck squamous cell carcinoma progression, Cancer Commun. 42 (2022) 223–244.
[36] J Ma, H Han, Y Huang, C Yang, S Zheng, T Cai, et al., METTL1/WDR4-mediated m7G tRNA modifications and m7G codon usage promote mRNA translation and lung cancer progression, Mol. Therapy 29 (2021) 3422–3435.
[37] Ying X, Liu B, Yuan Z, Jiang X, Zhang H, Qi D, et al. METTL1-m7G-EGFR/EFEMP1 axis promotes the bladder cancer development. 2021;22.
[38] L Li, Y Yang, Z Wang, C Xu, J Huang, G. Li, Prognostic role of METTL1 in glioma, Cancer Cell Int. 21 (2021) 633.
[39] Q-H Tian, M-F Zhang, J-S Zeng, R-G Luo, Y Wen, J Chen, et al., METTL1 overexpression is correlated with poor prognosis and promotes hepatocellular carcinoma via PTEN, J. Mol. Med. 97 (2019) 1535–1545.
[40] S Lin, Q Liu, VS Lelyveld, J Choe, JW Szostak, RI. Gregory, Mettl1/Wdr4-Mediated m7G tRNA Methylome is required for normal mRNA translation and embryonic stem cell self-renewal and differentiation, Mol. Cell 71 (2018) 244–255, e5.
[41] Z Dai, H Liu, J Liao, C Huang, X Ren, W Zhu, et al., N7-Methylguanosine tRNA modification enhances oncogenic mRNA translation and promotes intrahepatic cholangiocarcinoma progression, Mol. Cell 81 (2021) 3339–3355, e8.
[42] Y Zhao, L Kong, Z Pei, F Li, C Li, X Sun, et al., m7G Methyltransferase METTL1 promotes post-ischemic angiogenesis via promoting VEGFA mRNA translation, Front. Cell Dev. Biol. 9 (2021) 642080.
[43] CM Díaz-Montero, BI Rini, JH Finke, The immunology of renal cell carcinoma, Nat. Rev. Nephrol. 16 (2020) 721–735.
[44] JE Brown, K-L Royle, W Gregory, C Ralph, A Maraveyas, O Din, et al., Temporary treatment cessation versus continuation of first-line tyrosine kinase inhibitor in patients with advanced clear cell renal cell carcinoma (STAR): an open-label, non-inferiority, randomised, controlled, phase 2/3 trial, Lancet Oncol. 24 (2023) 213–227.
[45] Nakano O, Sato M, Naito Y, Suzuki K, Orikasa S, Aizawa M, et al. Proliferative Activity of Intratumoral CD8$^{+}$ T-Lymphocytes As a Prognostic Factor in Human Renal Cell Carcinoma: clinicopathologic demonstration of antitumor immunity.:5.
[46] J Cinier, M Hubert, L Besson, A Di Roio, C Rodriguez, V Lombardi, et al., Recruitment and expansion of Tregs cells in the tumor environment-how to target them? Cancers. (Basel) 13 (2021) 1850.
[47] RJ deLeeuw, SE Kost, JA Kakal, BH. Nelson, The prognostic value of FoxP3+ tumor-infiltrating lymphocytes in cancer: a critical review of the literature, Clin. Cancer Res. 18 (2012) 3022–3029.
[48] H Tao, Y Mimura, K Aoe, S Kobayashi, H Yamamoto, E Matsuda, et al., Prognostic potential of FOXP3 expression in non-small cell lung cancer cells combined with tumor-infiltrating regulatory T cells, Lung Cancer 75 (2012) 95–101.
[49] TJ Curiel, G Coukos, L Zou, X Alvarez, P Cheng, P Mottram, et al., Specific recruitment of regulatory T cells in ovarian carcinoma fosters immune privilege and predicts reduced survival, Nat. Med. 10 (2004) 942–949.
[50] EJ Sayour, P McLendon, R McLendon, G De Leon, R Reynolds, J Kresak, et al., Increased proportion of FoxP3+ regulatory T cells in tumor infiltrating lymphocytes is associated with tumor recurrence and reduced survival in patients with glioblastoma, Cancer Immunol. Immunther. 64 (2015) 419–427.
[51] Y Yan, L Huang, Y Liu, M Yi, Q Chu, D Jiao, et al., Metabolic profiles of regulatory T cells and their adaptations to the tumor microenvironment: implications for antitumor immunity, J. Hematol. Oncol. 15 (2022) 104.
[52] DA Fruman, H Chiu, BD Hopkins, S Bagrodia, LC Cantley, RT. Abraham, The PI3K Pathway in Human Disease, Cell 170 (2017) 605–635.
[53] C Xue, G Li, J Lu, L. Li, Crosstalk between circRNAs and the PI3K/AKT signaling pathway in cancer progression, Sig Transduct. Target Ther 6 (2021) 400.
[54] S Hu, X Zhang, H Xin, M Guo, Y Xiao, Z Chang, et al., Identification of PI3K-AKT Pathway-Related Genes and Construction of Prognostic Prediction Model for ccRCC, Cancer Rep. 7 (2024) e70010.